

Cite this: *RSC Pharm.*, 2026, **3**, 682

Controlled release of Ketoprofen via PLGA nanoparticles: an *in vitro* study for rheumatoid arthritis therapy

Soumen Samanta,^a Kazi Asraf Ali,^b Manas Bhowmik,^c Samir Das^a and Dipika Mandal^{b*}

Ketoprofen (KN) is one of the most commonly used non-steroidal anti-inflammatory drugs (NSAIDs). Low aqueous solubility and adverse gastrointestinal effects following oral dosing are the main challenges. Biodegradable polymers like PLGA (poly-(lactic-co-glycolic acid)) were utilized to develop nanoparticles for the controlled delivery of ketoprofen. Ketoprofen-loaded PLGA nanoparticles were made using the double emulsion solvent evaporation technique. We utilized Fourier transform infrared (FTIR) spectroscopy to determine the drug–excipient interactions. Particle size, zeta potential, encapsulation effectiveness, and drug-release patterns were also assessed for the produced nanoparticles. The nanoparticles exhibited average size ranges of 380–396 nm with negative zeta potentials, ensuring suspension stability. The encapsulation efficiency of formulation 3 (KN3) was observed to be over 95%, indicating effective drug loading. *In vitro* studies demonstrated a prolonged release of ketoprofen over a 120-hour period from the ketoprofen-loaded nanoparticles. The findings suggest that ketoprofen-loaded polymeric nanoparticles may serve as a viable method for tackling the associated challenges of conventional ketoprofen therapy. This study aimed to develop and characterize polymeric nanoparticles as an innovative drug delivery system for ketoprofen to achieve sustained drug release.

Received 23rd July 2025,
Accepted 26th November 2025

DOI: 10.1039/d5pm00196j

rsc.li/RSCPharma

Introduction

Arthritis is a devastating disease that occurs worldwide, and patients suffer from various systemic side effects from the treatment components, with debilitating adverse effects associated with the drugs used.^{1,2} Osteoarthritis (OA) and rheumatoid arthritis (RA) are treated with a variety of non-steroidal anti-inflammatory drugs (NSAIDs), such as diclofenac, naproxen, meloxicam, piroxicam and ketoprofen.^{3,4} Among them, ketoprofen is widely used for pain relief in arthritis, but because of its low water solubility and short half-life, about 1.5–2 h after oral administration,⁵ it requires frequent oral administration which causes gastrointestinal ulceration and bleeding.^{1,6} Ketoprofen is often formulated into nanoparticles to enhance its solubility, bioavailability, and therapeutic efficacy. Ketoprofen causes inhibition of the synthesis of pros-

taglandins (PGs) from arachidonic acid and reversible inhibition of cyclooxygenase (COX) enzyme.^{3,7,8}

Since the 1970s, drug-loaded nanoparticles have been used to decrease unwanted side effects and boost drug usage. These submicron-sized particles are more advantageous than conventional dosage forms. The main advantages of nanoparticles are enhanced solubility, reduced toxicity, improved efficacy, and increased ability to control drug delivery.^{5,9}

Various studies have been conducted on nanoparticles for the delivery of macromolecules like proteins, nucleic acids, peptides, small molecules and hormones.¹⁰ Polymeric nanoparticles have been extensively developed and offer a compelling substitute for the progressive and long-term delivery of therapeutic agents.¹¹ These nanoparticles prevent rapid drug release and provide sustained drug delivery, reducing the need for frequent administration. They also offer site-specific drug delivery opportunities.¹² Recently, polymeric nanoparticles have gained interest in the field of biomedical sciences. The size range of drug-loaded polymeric nanoparticles may be from 10 to 1000 nm.¹³ Polymeric nanoparticles are submicron-sized, solid drug-delivery systems with varying degrees of biodegradability. The formation of nanospheres or nanocapsules depends on the technique used to produce the nanoparticles.¹⁴ The drug may be dissolved, encapsulated, and dis-

^aDepartment of Pharmaceutical Technology, University of North Bengal, Darjeeling, West Bengal, PIN-734013, India

^bDepartment of Pharmaceutical Technology, Maulana Abul Kalam Azad University of Technology, West BengalNadia, PIN-741249, India.

E-mail: dipikamandal08@gmail.com, dipika.mandal@makautwb.ac.in

^cDepartment of Pharmaceutical Technology, Jadavpur University, Kolkata-700032, India



Table 1 Quantity of the drug and polymer used, actual drug loading, and percentage of entrapment efficiency of formulations

| Formulation code | Quantity of ketoprofen (mg) | Quantity of PLGA (mg) | Actual drug loading (%) (\pm SD) ^a | Entrapment efficiency (%) (\pm SD) ^a |
|------------------|-----------------------------|-----------------------|--|--|
| KN1 | 50 | 100 | 17.69 \pm 2.34 | 53.07 \pm 7.88 |
| KN2 | 100 | 100 | 39.19 \pm 4.85 | 78.38 \pm 6.78 |
| KN3 | 200 | 100 | 63.82 \pm 5.14 | 95.74 \pm 1.78 |

^a SD means standard deviation, $n = 3$.

persed to a nanoparticle matrix in nanospheres or nanocapsules. Nanoparticles have become an essential area of research in drug delivery.¹⁵ PLGA is mainly used to prepare the nanoparticles due to its greater stability, exceptional biocompatibility, biodegradability, and minimal immunogenicity. PLGA has been authorized by the US Food and Drug Administration (US-FDA) as a safe polymer for use in pharmaceutical applications. This polymer is used for the passive targeting of nanoparticles for accumulation in solid tumors.¹⁶ Numerous studies have been conducted on polymeric nanoparticles as drug carriers for a wide variety of diseases. Because of the process of “extravasation through leaky vasculature and subsequent inflammatory cell-mediated sequestration” (ELVIS), which is comparable to the enhanced permeability and retention (EPR) effect seen in tumors, NPs can also passively accumulate at sites of inflammation in arthritic tissues due to the increased permeability of vessels. Arthritis is a disease that depends on angiogenesis. Through the leaky vasculature at the site, polymeric NPs build up in the inflammatory synovium.^{17–20} Ketoprofen-loaded PLGA nanoparticles are a well-known formulation in drug delivery, largely because PLGA offers excellent biocompatibility, natural degradability, and flexible polymer characteristics.²¹

Our study aims to develop and evaluate polymeric nanoparticles of ketoprofen using various ratios of PLGA to enhance the solubility and to provide a sustained and controlled release, decreasing the required frequency of dosing and enhancing patient adherence to treatment.

Materials and methods

Intas Pharmaceuticals Ltd, Ahmedabad, gifted ketoprofen. Sigma-Aldrich Co. (Bengaluru, India) supplied PLGA (poly-D-L-lactide-co-glycolide; ratio 75 : 25; MW 66 000–107 000), whereas Hi-Media Pvt Ltd (West Bengal, India) supplied polyvinyl alcohol (PVA; MW 125 000). The supplier of dichloromethane (DCM) was Merck Life Science Private Limited. The remaining chemicals and reagents utilized were of analytical grade quality.

Formulation of nanoparticles containing ketoprofen

PLGA nanoparticles loaded with ketoprofen were made using a double emulsion solvent evaporation technique.^{16,22} Although ketoprofen is a hydrophobic drug and is generally well-suited for the single emulsion (O/W) method, we use the double

emulsion (W/O/W) technique to achieve specific formulation advantages, such as controlled release and improved encapsulation. The double emulsion method can slow down the diffusion of ketoprofen from the nanoparticles, as the additional aqueous layer acts as a diffusion barrier. This can be beneficial for prolonged or sustained-release formulations.²³ For this technique, two aqueous phases and one organic phase were prepared. First, aqueous solutions containing 1.5% w/v and 2.5% w/v PVA were made. The drug, PLGA, and dichloromethane (2 ml) were used to prepare the oil phase. Table 1 shows the various quantities of ketoprofen and PLGA used in the nanoparticle preparations. A 1.5% w/v PVA solution (0.5 ml) was added to the drug polymer containing the organic phase with continuous homogenization at high speed, 20 000 rpm for 5 min (IKA Ultra Turrax T-10 Basic, Staufen, Germany), to prepare the primary emulsion (w/o).²⁴ The obtained primary emulsion was gradually incorporated into 75 ml of 2.5% w/v aqueous PVA mixture and homogenized at the same speed for 8 min. Higher PVA concentrations generally increase the viscosity of the aqueous phase, which can reduce particle coalescence during emulsification and lead to smaller and more uniform nanoparticles. The molecular weight and degree of hydrolysis of PVA were 89 000–98 000 and 99+%, respectively. PVA with a higher molecular weight provides better steric stabilization by forming a thicker adsorbed layer around the nanoparticles.²⁵ This can enhance colloidal stability and prevent aggregation. The degree of hydrolysis determines the number of hydroxyl groups available on the PVA chains. A higher degree of hydrolysis increases hydrogen bonding with the particle surface, improving stabilization and the zeta potential.²⁶ The organic solvent was evaporated by placing the formed mixture in a magnetic stirrer overnight. After producing the double emulsion, the organic solvent must be completely removed to harden the nanoparticles and ensure safety. Although DCM is volatile (boiling point 39.6 °C), its complete removal from an aqueous emulsion system is slow, requiring prolonged, often overnight, stirring.²⁷ The polyvinyl alcohol used in the formulation plays a vital role in preventing nanoparticle agglomeration during overnight solvent evaporation. PVA lowers the interfacial tension between the organic and aqueous phases. Smaller, more stable droplets are formed, which resist coalescence during solvent evaporation. Processing for 3 hours at 37 °C will remove a lot of free DCM, but it is insufficient to fully remove DCM that is emulsified, trapped inside polymer droplets/particles, or absorbed into the polymer matrix.²⁸ After that, using a cold centrifuge (Z32HK,



Hermle Labortechnik GmbH, Germany), the nanoparticles were separated and washed.²⁹ At first, the target temperature was set to 4 °C. Centrifuge tubes should be loaded symmetrically to ensure balance. The nanoparticles were separated at 15 000 rpm for 45 min and washed three times at 15 000 rpm for 10 min with double-distilled water to eliminate unbound drug and PVA.³⁰ The separated nanoparticles were placed at -40 °C in a Petri dish overnight. The next day, the cold formulations were dried using a freeze dryer (Laboratory Freeze Dryer, Labogene Scandinavian by Design, Assam, India) for eight hours.³¹ The dried nanoparticles were ultimately gathered and stored in a refrigerator at 4 °C for future use. We also prepared a blank nanoparticle formulation without adding the drug using a method similar to the one mentioned.^{32,33}

FTIR (Fourier transform infrared) spectroscopy

FTIR spectroscopy is a vital analytical technique used to identify and analyze the chemical bonds and functional groups present in sample materials. The infrared spectra were observed using an FTIR spectrophotometer (Bruker Alpha-II, Labindia Analytical Instrument Pvt. Ltd India) by the KBr pellet approach, operating in the wavelength range between 4000 and 400 cm⁻¹. The spectra obtained for ketoprofen, PVA, PLGA, their physical mixtures, and the nanoparticle formulation (KN3) were compared to observe the compatibility of the drug with polymers.^{34,35}

Physicochemical characterization of nanoparticles

Percentage entrapment efficiency. First, the required quantity of ketoprofen-loaded nanoparticles was accurately weighed and placed into a 2 ml Eppendorf tube. A prepared acetonitrile-water mixture (50 : 50) was added to that tube. Then, it was sonicated for a few hours and centrifuged at 10 000 rpm for 10 min. The supernatant was collected, and the absorbance of the sample was measured using a UV spectrophotometer.³⁶ The absorbance of the blank formulation was also measured using the same procedure. All analyses were performed in triplicate.³⁷ The following formulas were used to determine the percentage entrapment efficiency:

$$\begin{aligned} & \text{Percentage of actual drug loading} \\ &= \frac{\text{amount of drug present in nanoparticles}}{\text{weight of nanoparticle sample analysed}} \times 100 \quad (1) \end{aligned}$$

$$\begin{aligned} & \text{Percentage of loading efficiency} \\ &= \frac{\text{actual drug loading}}{\text{theoretical drug loading}} \times 100. \quad (2) \end{aligned}$$

Size metrics, range of particle sizes, and surface charge. Assessing the particle size distribution allows inference of the nanoparticles' mean size range. The zeta potential determines the stability of the colloidal dispersion and quantifies the surface charge of particles.³⁸ Measurements of the zeta potential and particle size spread were carried out with the help of a zetasizer (Litesizer Series 500, Anton Paar India Pvt. Ltd, India). Before analysis, a small amount of material was dis-

solved in deionized (DI) water. A plastic cuvette was used for particle size distribution, and an omega cuvette was used for zeta potential determination.³⁹

Surface morphology of nanoparticles. Surface morphology refers to the study and description of the surface structure and topography of nanoparticles, including their texture, roughness, and overall shape. The surface morphology of the generated nanoparticles was ascertained by scanning electron microscopy (SEM) (model-JSM-IT100, JEOL Ltd, Tokyo, Japan). Before observation, a gold layer was applied to the nanoparticles using vacuum coating.^{40,41} A small amount of dried nanoparticles was mounted onto an aluminum stub using conductive carbon tape to secure the particles. To prevent charging effects during imaging, the samples were sputter-coated with a thin layer of gold under vacuum. This coating enhances the electrical conductivity of the sample surface and improves image resolution and contrast. SEM analysis requires a vacuum value of 10⁻² Pa and a duration of around 3–5 minutes under optimal conditions.⁴²

In vitro release studies. For the *in vitro* release studies, phosphate-buffered saline (PBS) with a pH of 7.4 was used. The required amount (2 mg) of the prepared nanoparticles was placed in an Eppendorf tube containing PBS. An incubator shaker held the container and agitated it at 37 ± 0.5 °C. The tubes were taken out of the incubator shaker at scheduled times (*e.g.*, 0.5, 1, 2, 3, 4, 5, 6, 12, 24, 48, 72, and 120 hours) and centrifuged for 10 minutes at 10 000 rpm. A 1 ml sample of the supernatant was removed from the tube, and the nanoparticles were re-suspended and incubated under the same conditions as before.⁴³ Immediately, a corresponding volume of fresh PBS was used to replace the removed sample, maintaining a consistent volume in the dissolution fluid. The absorbance of the obtained sample's supernatant was analyzed using a UV-vis spectrophotometer at 260 nm against fresh PBS (pH 7.4) as the blank. The concentration of released ketoprofen in each sample was determined by referencing the standard curve. The method was performed three times to confirm the reproducibility.^{44,45}

Results and discussion

FTIR study

To evaluate drug-excipient interactions, FTIR spectral analysis was performed. Fig. 1 illustrates the drug-excipient interaction study, comparing pure drug, the excipients used, the physical mixture, and the nanoparticle formulation. The FTIR spectrum of ketoprofen exhibited a characteristic peak at 2877 cm⁻¹, corresponding to C-H stretching. It also showed peaks at 1696 cm⁻¹ and 1654 cm⁻¹ due to the symmetric stretching vibrations of the carboxyl and ketone groups. The FTIR spectra of PLGA exhibited a characteristic peak around 3500 cm⁻¹ for O-H stretching and peaks at 2995.53 cm⁻¹ and 2945.45 cm⁻¹ for C-H stretching. A peak at 866 cm⁻¹ is for C-C stretching. The FTIR spectra of PVA showed peaks for O-H stretching at 3463.14 cm⁻¹, C-H stretching at 2925 cm⁻¹, and C-O stretch-



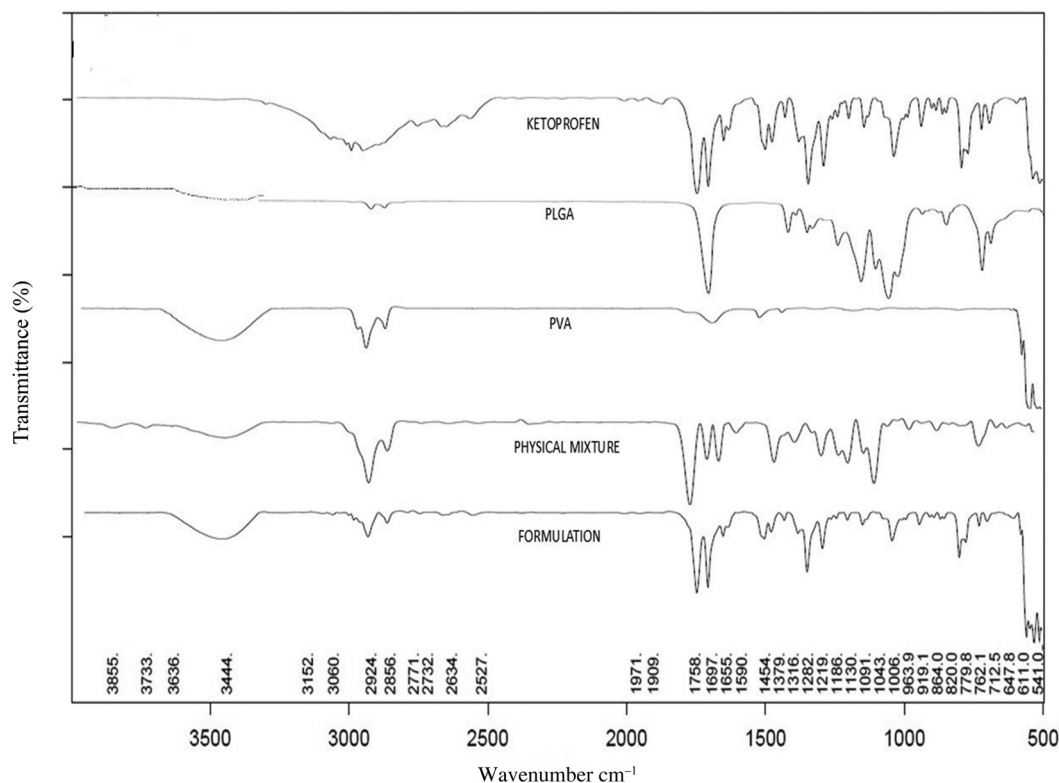


Fig. 1 FTIR spectra of ketoprofen, PLGA, PVA, physical mixture, and nanoparticle.

ing vibrations at 1143 cm^{-1} .⁴⁶ It was found that the physical mixture of the medication, PVA, and PLGA included all of their characteristic peaks. In the formulation spectrum, characteristic peaks at $3500\text{--}3000\text{ cm}^{-1}$ for hydroxyl groups of PVA and possibly the carboxylic O–H of ketoprofen, a peak at 1758 cm^{-1} for PLGA's ester carbonyl ($-\text{C}(=\text{O})-\text{O}-$), a peak at 1697 cm^{-1} for C=O stretching of ketoprofen, peaks at $1655\text{--}1590\text{ cm}^{-1}$ for C=C stretching of the drug, peaks at $1454\text{--}1379\text{ cm}^{-1}$ for C–H bending of the drug and polymers, peaks at $1283\text{--}1186\text{ cm}^{-1}$ for C–O–C stretching of ester linkages in PLGA and PVA, peaks at $1130\text{--}1043\text{ cm}^{-1}$ for C–O stretching from PVA and PLGA and peaks at $960\text{--}760\text{ cm}^{-1}$ for C–H bending from ketoprofen aromatic structure were observed.⁴⁷ Double-headed bands were observed between 1758 and 1697 cm^{-1} , which correspond to overlapping carbonyl (C=O) stretching vibrations of both the polymer (ester C=O) and ketoprofen (carboxylic C=O). The persistence of the ketoprofen carbonyl peak indicates that the drug remains intact in the formulation. However, the broadening and partial merging of these peaks suggest physical interactions.⁴⁸ The characteristic ketoprofen C=O stretching band at 1696 cm^{-1} is present in the pure ketoprofen spectrum. In the formulation spectrum, the corresponding band appears at 1697 cm^{-1} but with noticeably reduced intensity and some broadening. The wavenumber difference (0.4 cm^{-1}) is negligible and therefore not a meaningful shift, but the reduction in intensity/increased bandwidth is clear. The reduced intensity and broadening of the

C=O band in the formulation indicate that the ketoprofen carbonyl is interacting with the formulation matrix, which may be due to hydrogen bonding.⁴⁹ From this study, it can be concluded that the drug and the excipients do not exhibit any chemical interactions.⁵⁰

Loaded drug content and corresponding efficiency

The study found that drug loading efficiency gradually increased as the quantity increased. It was optimum at a drug : polymer ratio of 2 : 1. The actual drug loading values of the formulations KN1, KN2, and KN3 were $17.69 \pm 2.34\%$, $39.19 \pm 4.85\%$, and $63.82 \pm 5.14\%$, respectively. The percentage values of loaded drug effectiveness of the above formulations were $53.07 \pm 7.88\%$, $78.38 \pm 6.78\%$, and $95.74 \pm 1.78\%$, respectively, as presented in Table 1. The highest percentage of drug loading was seen in KN3. With increasing amount of drug, drug loading and loading efficiency were increased.⁴⁹ Maximizing drug loading and loading efficiency in ketoprofen nanoparticles is essential for developing an effective system for drug administration.^{51,52}

Particle size and associated surface potential

The mean particle sizes of the prepared formulations were $396 \pm 13.5\text{ nm}$, $383.9 \pm 7.9\text{ nm}$, and $380.4 \pm 5.4\text{ nm}$, respectively. The polydispersity indexes of KN1, KN2 and KN3 were 0.253 ± 0.010 , 0.248 ± 0.08 and 0.233 ± 0.04 , and the zeta potentials of the prepared formulations were -8.6 ± 1.52 , -8.9 ± 0.88 and



Table 2 Mean particle size, polydispersity index, and zeta potential of nanoparticles

| Formulation code | Mean particle size (nm) ^a | Polydispersity index ^a | Zeta potential (mV) ^a |
|------------------|--------------------------------------|-----------------------------------|----------------------------------|
| KN1 | 389.4 ± 13.5 | 0.253 ± 0.010 | -8.6 ± 1.52 |
| KN2 | 383.9 ± 7.9 | 0.248 ± 0.08 | -8.9 ± 0.88 |
| KN3 | 380.4 ± 5.4 | 0.233 ± 0.04 | -9.3 ± 0.78 |

^a Data are shown in mean ± standard deviation ($n = 3$).

-9.3 ± 0.78, respectively, as shown in Table 2. The prepared nanoparticle sizes were below 500 nm. Optimizing the particle size of ketoprofen-loaded PLGA nanoparticles is crucial for maximizing therapeutic efficacy. Smaller, uniformly sized nanoparticles can provide a more consistent and controlled release of ketoprofen, potentially reducing the dosing frequency.^{53,54} The PDI specifies the homogeneity of the nanoparticles and describes the size distribution. The nanoparticles showed a low PDI (close to 0), indicating a narrow size distribution,

which is often desirable for uniform drug release and consistent biological behavior.⁵⁵ The zeta potential values for the ketoprofen nanoparticles suggest moderate stability and a reasonably consistent formulation process. Such low zeta potential values suggest that the nanoparticles are only marginally stable in suspension, so special care is needed to maintain their stability over time. Storing nanoparticles at lower temperatures can slow down the kinetic energy of the particles, reducing the likelihood of aggregation. Refrigeration can be an effective way to prolong the stability of nanoparticles with low zeta potential (Fig. 2 and 3).^{56,57}

SEM study

The morphological study of the prepared formulations was conducted using SEM. The developed nanoparticles exhibited a spherical shape with a smooth surface (Fig. 4). Smooth surfaces may indicate a homogeneous distribution of the drug and excipients. Uniform spherical particles are often desirable for controlled release and predictable pharmacokinetics.^{58,59}

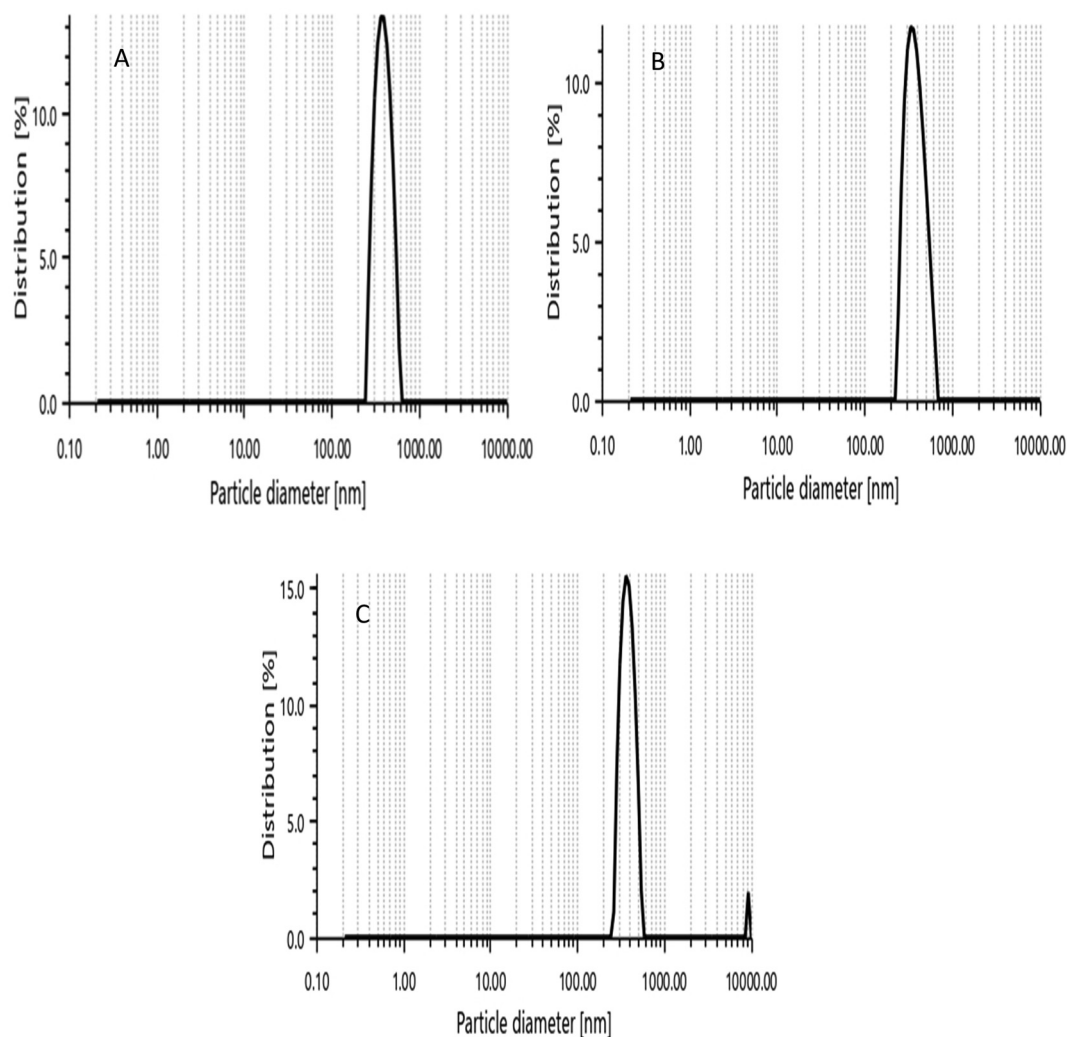


Fig. 2 Particle size distribution of different formulations: (A) KN1, (B) KN2, and (C) KN3.



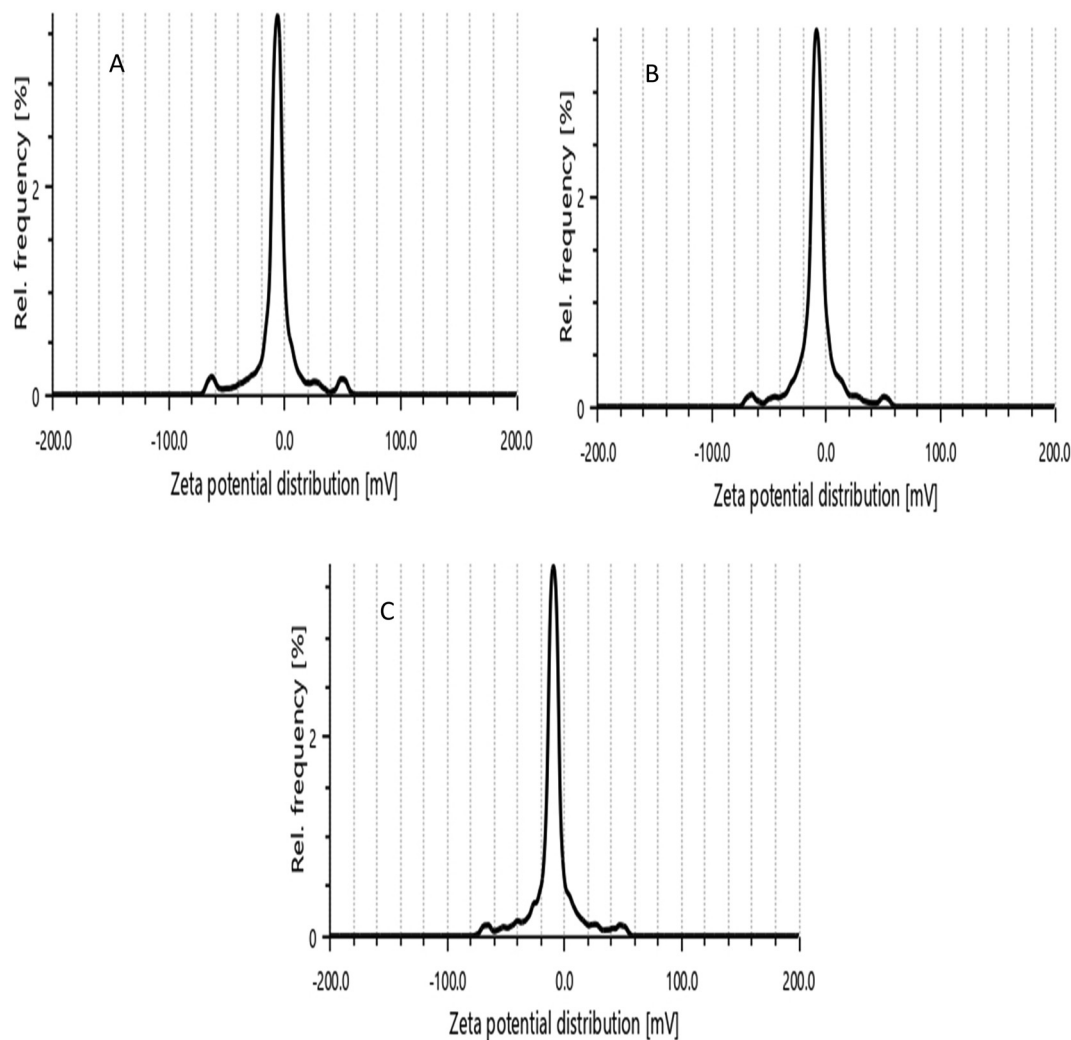


Fig. 3 Zeta potential of different formulations: (A) KN1, (B) KN2, and (C) KN3.

Studies on *in vitro* drug release

Fig. 5 presents the results of the *in vitro* release study for the formulations. The result shows a dual drug release pattern. Initially, there are burst releases and then continuous sustained drug release profiles. The first burst release could result from the medication dissolving on the nanoparticle surface, and the drug may continuously diffuse from the particle core, causing a continual release. During nanoparticle formulation, a portion of the drug may attach to or become confined around the particle's surface rather than being incorporated into the core. When these nanoparticles are introduced into the release medium, the drug located on the surface dissolves rapidly, resulting in the burst release.⁶⁰ After 120 hours of the drug release study in KN1, KN2, and KN3, the cumulative percentages of drug released were $96.778 \pm 5.02\%$, $56.545 \pm 4.45\%$, and $38.26 \pm 3.12\%$, respectively. The cumulative percentage of drug release from KN3 was slower than that from KN2 and KN1.⁶¹ Ketoprofen has low solubility in water and phos-

phate buffer. PLGA (75 : 25) is also a highly non-polar polymer. Hence, drug release from the formulation was very slow.

Although several studies have reported ketoprofen-loaded PLGA nanoparticles,^{20,62–65} the present study is distinct in its use of the double-emulsion solvent evaporation method with PVA as a stabilizer, resulting in high encapsulation efficiency (95%), a particle size of 380 nm, and sustained release for 120 h following Fickian diffusion (Korsmeyer–Peppas model, $n \leq 0.45$). Compared with previous works, our formulation achieved superior encapsulation and longer release (*vs.* 40–78% and shorter durations in earlier studies). Unlike Kluge *et al.* (2009), who used SFEE,⁶³ and Shah *et al.* (2011), who targeted topical co-delivery systems, our study focused on systemic, prolonged release.⁶⁴ Similarly, Elmaskaya *et al.* (2019) and Varga *et al.* (2023) obtained lower efficiency (14–78%) and shorter release (≤ 7 h), while our optimized KN3 formulation maintained controlled release for up to 120 h. Thus, this study presents a notable advancement by combining double-emulsion processing and optimized PVA stabilization to achieve



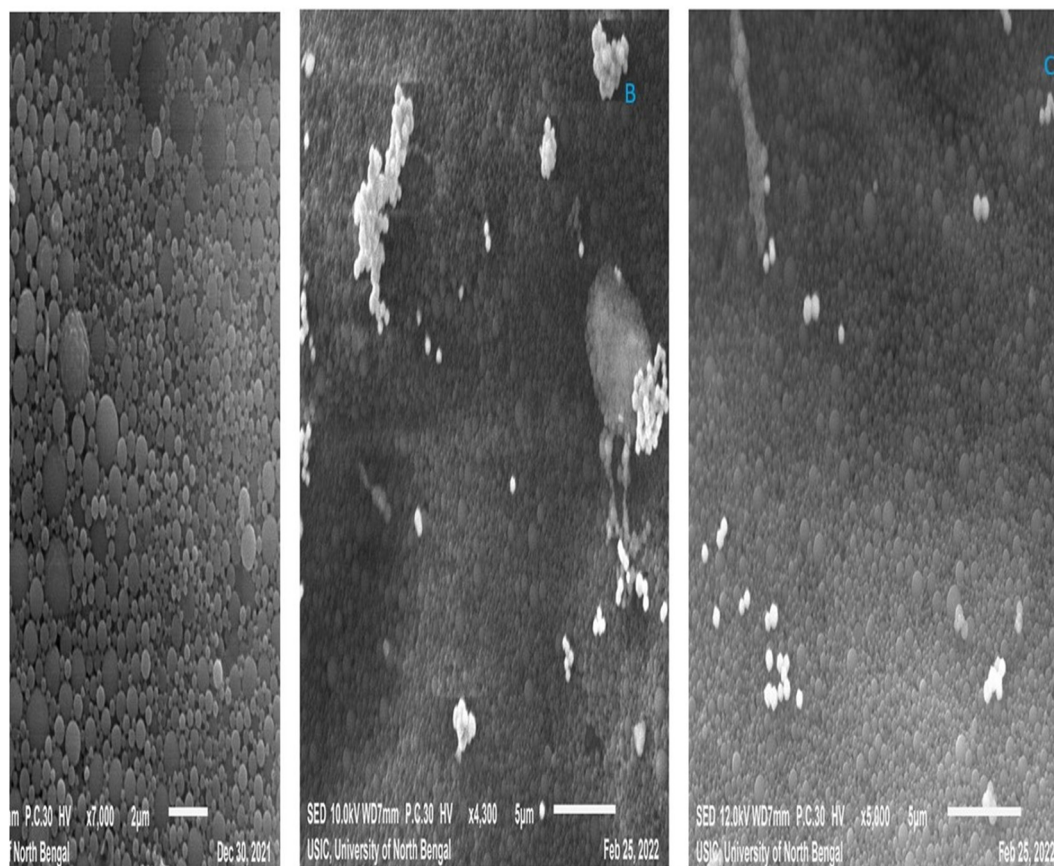


Fig. 4 SEM images of different formulations: (A) KN1, (B) KN2, and (C) KN3.

enhanced encapsulation and prolonged drug release suitable for rheumatoid arthritis therapy.^{65,65}

The release exponent “ n ” and correlation coefficient (R^2) were calculated using the different drug release kinetic models examined for the experimental formulations (where appropriate), as shown in Table 3. Data on drug release for the various formulations were analyzed using multiple kinetic models. KN1 demonstrated strong linearity in the first-order kinetic model ($R^2 = 0.9406$). At the same time, KN2 and KN3 exhibited good linearity in the Korsmeyer–Peppas kinetic model, with R^2 values of 0.9848 and 0.9901, respectively, compared to other models.⁶⁶

The term “release exponent” (denoted as n) is commonly used in the context of mechanisms of drug release from controlled-release formulations. Specifically, it appears in the Korsmeyer–Peppas equation, which models the kinetics of drug release from various pharmaceutical delivery systems. $M_t/M_\infty = Kt^n$ is the equation, where M_t/M_∞ is the proportion of the drug released at time t , and n is the release exponent, indicating the drug release method. An n value of ≤ 0.45 signifies Fickian diffusion, where the concentration gradient between the nanoparticle core and the surrounding environment primarily drives the drug release.^{61,67} An “ n ” value ranging from 0.45 to 0.89 suggests non-Fickian or anomalous transport,

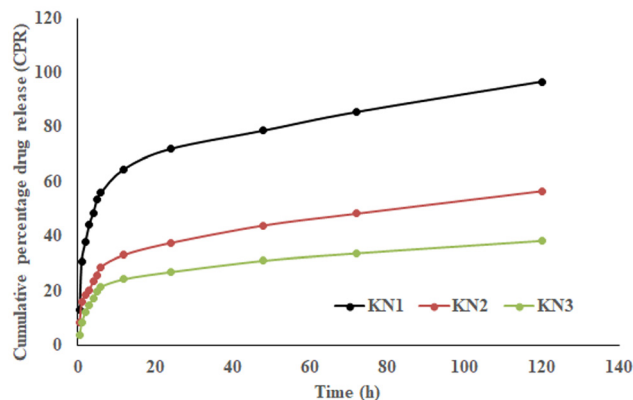


Fig. 5 *In vitro* release profiles of KN1, KN2, and KN3.

meaning that the drug’s diffusion and the nanoparticle matrix’s relaxation (swelling or structural rearrangement) contribute to the overall release. When $n = 0.89$, the drug release is consistent with Case-II transport, which is associated with polymer relaxation or erosion. In our formulations, $n \leq 0.45$.^{68,69} For spherical nanoparticles, drug diffusion through the matrix follows Fick’s law, which is typical for small mole-



Table 3 *In vitro* release kinetics, including R^2 and “ n ” values for different preparations

| <i>In vitro</i> release kinetics | KN1 | KN2 | KN3 |
|----------------------------------|---|--|--|
| Zero-order kinetics | $y = 0.2929x + 39.653$ $R^2 = 0.6364$ | $y = 0.1833x + 19.667$ $R^2 = 0.7519$ | $y = 0.1263x + 13.688$ $R^2 = 0.6683$ |
| First-order kinetics | $y = -0.0052x + 1.8009$ $R^2 = 0.9406$ | $y = -0.0013x + 1.9047$ $R^2 = 0.8434$ | $y = -0.0007x + 1.9351$ $R^2 = 0.7289$ |
| Higuchi kinetics | $y = 0.0494x + 1.3943$ $R^2 = 0.53$ | $y = 0.052x + 1.1044$ $R^2 = 0.6413$ | $y = 0.0585x + 0.8866$ $R^2 = 0.558$ |
| Korsmeyer–Peppas kinetics | $y = 0.3521x + 1.2678$ $R^2 = 0.8497$ $n = 0.352$ | $y = 0.0532x - 0.4204$ $R^2 = 0.9848$ $n = 0.0532$ | $y = 0.073x - 0.3486$ $R^2 = 0.9901$ $n = 0.073$ |
| Hixson–Crowell kinetics | $y = -0.0108x + 3.9336$ $R^2 = 0.8699$ | $y = -0.0038x + 4.3138$ $R^2 = 0.8144$ | $y = -0.0023x + 4.4171$ $R^2 = 0.7089$ |

cules that can quickly move through the nanoparticle matrix without structural changes to the carrier. This mechanism is common in non-swelling nanoparticles where the drug diffuses without changing the nanoparticle structure.^{67,70} However, such a low exponent suggests that diffusion is extremely restricted, possibly due to strong drug entrapment within the PLGA matrix. In polymeric systems like PLGA, the release process is typically governed by a combination of diffusion through the polymer network and polymer degradation or erosion.⁷¹ If the diffusion exponent is significantly below 0.45, it could imply that drug mobility within the polymer is severely hindered, perhaps due to dense polymer packing, high PLGA molecular weight, or strong hydrogen bonding between ketoprofen and the polymer. Additionally, since PVA was used as a stabilizer, residual PVA adsorption could form a barrier around the nanoparticles, further slowing drug diffusion and leading to an anomalously low n value.

Conclusion

The double-emulsion solvent evaporation method was found to be an efficient technique for preparing PLGA nanoparticles containing ketoprofen, an NSAID used for pain and inflammation in rheumatoid arthritis. The developed nanoparticles were in the nanometer size range, exhibiting uniform spherical morphology with smooth surfaces, desirable attributes for efficient drug delivery and cellular uptake. KN3 demonstrated superior performance among the formulations studied, exhibiting the highest entrapment efficiency and a more precise and persistent drug release profile in contrast to KN1 and KN2. This suggests that optimizing formulation parameters can significantly influence the nanoparticles' release kinetics and therapeutic potential.

Our findings highlight the potential of ketoprofen-loaded PLGA nanoparticles as a biodegradable and biocompatible system for sustained drug delivery, aiming to reduce the dosing interval and minimize systemic adverse reactions commonly associated with oral NSAIDs. However, while the *in vitro* characterization results are encouraging, further comprehen-

sive studies are essential to realize this delivery system's clinical potential fully. Future research should emphasize detailed *in vivo* evaluations to explore the pharmacokinetics, pharmacodynamic behaviors, long-term safety, and therapeutic efficacy in appropriate animal models. Additionally, scaling up the production process while ensuring reproducibility, stability, and regulatory compliance will be crucial for translation from bench to bedside.

Ethical statement

This study did not involve animal or human volunteers.

Author contributions

S. S. writing – original draft, methodology, and investigation; K. A. A. writing – review and editing; M. B. writing – review and editing; S. D. writing – review and editing; D. M. conceptualization, visualization, editing, and supervision.

Conflicts of interest

The authors have no conflict of interests to disclose.

Data availability

The datasets produced and/or analyzed during this study can be obtained by making a reasonable request to the author of the correspondence.

Acknowledgements

We affirm that this study was not supported by external funding. We appreciate the kind gift sample of ketoprofen that was sent to us by Intas Pharmaceuticals Ltd in Ahmedabad.



References

- 1 R. Gul, N. Ahmed, N. Ullah, M. I. Khan, A. Elaissari and Asim ur Rehman, . Biodegradable ingredient-based emulgel loaded with ketoprofen nanoparticles, *AAPS PharmSciTech*, 2018, **19**(4), 1869–1881. Available from: <https://link.springer.com/10.1208/s12249-018-0997-0>.
- 2 A. F. Radu and S. G. Bungau, Management of rheumatoid arthritis: An overview, *Cells*, 2021, **10**(11), 2857. Available from: <https://www.mdpi.com/2073-4409/10/11/2857>.
- 3 N. Nagai, A. Iwamae, S. Tanimoto, C. Yoshioka and Y. Ito, Pharmacokinetics and antiinflammatory effect of a novel gel system containing ketoprofen solid nanoparticles, *Biol. Pharm. Bull.*, 2015, **38**(12), 1918–1924. Available from: https://www.jstage.jst.go.jp/article/bpb/38/12/38_b15-00567/_article.
- 4 G. Iolascon, S. Giménez and D. Mogyorósi, A review of aceclofenac: Analgesic and anti-inflammatory effects on musculoskeletal disorders, *J. Pain Res.*, 2021, **14**, 3651–3663. Available from: <https://www.dovepress.com/a-review-of-aceclofenac-analgesic-and-anti-inflammatory-effects-on-muscle-peer-reviewed-fulltext-article-JPR>.
- 5 K. Betlejewska-Kielak, E. Bednarek, A. Budzianowski, K. Michalska and J. K. Maurin, Comprehensive characterisation of the ketoprofen- β -cyclodextrin inclusion complex using X-ray techniques and NMR spectroscopy, *Molecules*, 2021, **26**(13), 4089. Available from: <https://www.mdpi.com/1420-3049/26/13/4089>.
- 6 R. Soto, M. Svård, V. Verma, L. Padrela, K. Ryan and Å. C Rasmuson, Solubility and thermodynamic analysis of ketoprofen in organic solvents, *Int. J. Pharm.*, 2020, **588**, 119686. Available from: <https://linkinghub.elsevier.com/retrieve/pii/S0378517320306700>.
- 7 J. Khan, S. Bashir, M. A. Khan, R. Ghaffar, A. Naz, W. Khan, *et al.*, Enhanced dissolution rate of ketoprofen by fabricating into smart nanocrystals, *Pak. J. Pharm. Sci.*, 2019, **32**(6 (Supplementary)), 2899–2904.
- 8 N. Halfter, E. Espinosa-Cano, G. M. Pontes-Quero, R. A. Ramírez-Jiménez, C. Heinemann, S. Möller, *et al.*, Ketoprofen-based polymer-drug nanoparticles provide anti-inflammatory properties to HA/collagen hydrogels, *J. Funct. Biomater.*, 2023, **14**(3), 160. Available from: <https://www.mdpi.com/2079-4983/14/3/160>.
- 9 T. C. Ezike, U. S. Okpala, U. L. Onoja, C. P. Nwike, E. C. Ezeako, O. J. Okpara, *et al.*, Advances in drug delivery systems, challenges and future directions, *Heliyon*, 2023, **9**(6), e17488. Available from: <https://linkinghub.elsevier.com/retrieve/pii/S2405844023046960>.
- 10 S. Hong, D. W. Choi, H. N. Kim, C. G. Park, W. Lee and H. H. Park, Protein-based nanoparticles as drug delivery systems, *Pharmaceutics*, 2020, **12**(7), 604. Available from: <https://www.mdpi.com/1999-4923/12/7/604>.
- 11 L. Jia, P. Zhang, H. Sun, Y. Dai, S. Liang, X. Bai, *et al.*, Optimization of nanoparticles for smart drug delivery: A review, *Nanomaterials*, 2021, **11**(11), 2790. Available from: <https://www.mdpi.com/2079-4991/11/11/2790>.
- 12 K. Singh, S. Singhal, S. Pahwa, V. A. Sethi, S. Sharma, P. Singh, *et al.*, Nanomedicine and drug delivery: A comprehensive review of applications and challenges, *Nano-Struct. Nano-Objects*, 2024, **40**, 101403. Available from: <https://linkinghub.elsevier.com/retrieve/pii/S2352507X24003159>.
- 13 A. Yusuf, A. R. Z. Almotairy, H. Henidi, O. Y. Alshehri and M. S. Aldughaim, Nanoparticles as drug delivery systems: A review of the implication of nanoparticles' physicochemical properties on responses in biological systems, *Polymers*, 2023, **15**(7), 1596. Available from: <https://www.mdpi.com/2073-4360/15/7/1596>.
- 14 A. Zielińska, F. Carreiró, A. M. Oliveira, A. Neves, B. Pires, D. N. Venkatesh, *et al.*, Polymeric nanoparticles: Production, characterization, toxicology and ecotoxicology, *Molecules*, 2020, **25**(16), 3731. Available from: <https://www.mdpi.com/1420-3049/25/16/3731>.
- 15 O. Afzal, A. S. A. Altamimi, M. S. Nadeem, S. I. Alzarea, W. H. Almalki, A. Tariq, *et al.*, Nanoparticles in drug delivery: From history to therapeutic applications, *Nanomaterials*, 2022, **12**(24), 4494. Available from: <https://www.mdpi.com/2079-4991/12/24/4494>.
- 16 D. Mandal, T. K. Shaw, G. Dey, M. M. Pal, B. Mukherjee, A. K. Bandyopadhyay, *et al.*, Preferential hepatic uptake of paclitaxel-loaded poly-(d-l-lactide-co-glycolide) nanoparticles—A possibility for hepatic drug targeting: Pharmacokinetics and biodistribution, *Int. J. Biol. Macromol.*, 2018, **112**, 818–830. Available from: <https://linkinghub.elsevier.com/retrieve/pii/S0141813017335778>.
- 17 T. Ishihara, T. Kubota, T. Choi and M. Higaki, Treatment of experimental arthritis with stealth-type polymeric nanoparticles encapsulating betamethasone phosphate, *J. Pharmacol. Exp. Ther.*, 2009, **329**(2), 412–417. Available from: <https://linkinghub.elsevier.com/retrieve/pii/S0022356524384083>.
- 18 A. E. Koch, Angiogenesis as a target in rheumatoid arthritis, *Ann. Rheum. Dis.*, 2003, **62**, ii60–ii67. Available from: <https://linkinghub.elsevier.com/retrieve/pii/S000349672443447X>.
- 19 H. Maeda, J. Wu, T. Sawa, Y. Matsumura and K. Hori, Tumor vascular permeability and the EPR effect in macromolecular therapeutics: a review, *J. Controlled Release*, 2000, **65**(1–2), 271–284. Available from: <https://linkinghub.elsevier.com/retrieve/pii/S0168365999002485>.
- 20 M. Zhao, J. Yao, X. Meng, Y. Cui, T. Zhu, F. Sun, *et al.*, Polyketal nanoparticles co-loaded with miR-124 and ketoprofen for treatment of rheumatoid arthritis, *J. Pharm. Sci.*, 2021, **110**(5), 2233–2240. Available from: <https://linkinghub.elsevier.com/retrieve/pii/S0022354921000666>.
- 21 K. A. Kravanja, K. Khanari, M. K. Marevci, U. Maver and M. Finšgar, Ketoprofen-loaded PLGA-based bioactive coating prepared by supercritical foaming on a TiAl6V4 substrate for local drug delivery in orthopedic applications, *Prog. Org. Coat.*, 2024, **186**, 108026. Available from: <https://linkinghub.elsevier.com/retrieve/pii/S0300944023006227>.
- 22 J. Mosafer, K. Abnous, M. Tafaghodi, A. Mokhtarzadeh and M. Ramezani, In vitro and in vivo evaluation of anti-nucleo-



- lin-targeted magnetic PLGA nanoparticles loaded with doxorubicin as a theranostic agent for enhanced targeted cancer imaging and therapy, *Eur. J. Pharm. Biopharm.*, 2017, **113**, 60–74. Available from: <https://linkinghub.elsevier.com/retrieve/pii/S0939641116309651>.
- 23 F. Otto and A. Froelich, Microemulsion-based polymer gels with ketoprofen and menthol: Physicochemical properties and drug release studies, *Gels*, 2024, **10**(7), 435. Available from: <https://www.mdpi.com/2310-2861/10/7/435>.
- 24 K. Kizilbey, Optimization of rutin-loaded PLGA nanoparticles synthesized by single-emulsion solvent evaporation method, *ACS Omega*, 2019, **4**(1), 555–562. Available from: <https://pubs.acs.org/doi/10.1021/acsomega.8b02767>.
- 25 J. L. Patarroyo, J. Cifuentes, L. N. Muñoz, J. C. Cruz and L. H. Reyes, Novel antibacterial hydrogels based on gelatin/polyvinyl-alcohol and graphene oxide/silver nanoconjugates: formulation, characterization, and preliminary biocompatibility evaluation, *Heliyon*, 2022, **8**(3), e09145. Available from: <https://linkinghub.elsevier.com/retrieve/pii/S2405844022004339>.
- 26 M. C. Alvarado, Recent progress in polyvinyl alcohol (PVA)/nanocellulose composite films for packaging applications: A comprehensive review of the impact on physico-mechanical properties, *Food Bioeng.*, 2024, **3**(2), 189–209. Available from: <https://onlinelibrary.wiley.com/doi/10.1002/fbe2.12086>.
- 27 N. J. Caggiano, M. S. Armstrong, J. S. Georgiou, A. Rawal, B. K. Wilson, C. E. White, *et al.*, Formulation and scale-up of delamanid nanoparticles via emulsification for oral tuberculosis treatment, *Mol. Pharmaceutics*, 2023, **20**(9), 4546–4558. Available from: <https://pubs.acs.org/doi/10.1021/acs.molpharmaceut.3c00240>.
- 28 Z. Liu, O. L. Lanier and A. Chauhan, Poly (vinyl alcohol) assisted synthesis and anti-solvent precipitation of gold nanoparticles, *Nanomaterials*, 2020, **10**(12), 2359. Available from: <https://www.mdpi.com/2079-4991/10/12/2359>.
- 29 P. Gautam, M. H. Akhter, A. Anand, S. O. Rab, M. Jaremko and A. H. Emwas, Mesalamine loaded ethyl cellulose nanoparticles: Optimization and in vivo evaluation of anti-oxidant potential in ulcerative colitis, *Biomed. Mater.*, 2025, **20**(1), 015008. Available from: <https://iopscience.iop.org/article/10.1088/1748-605X/ad920e>.
- 30 A. Kumar Sahdev, C. J. Raorane, M. A. Ali, K. Mashay Al-Anazi, R. K. Manoharan, V. Raj, *et al.*, Chitosan-folic acid-coated quercetin-loaded PLGA nanoparticles for hepatic carcinoma treatment, *Polymers*, 2025, **17**(7), 955. Available from: <https://www.mdpi.com/2073-4360/17/7/955>.
- 31 G. Degobert and D. Aydin, Lyophilization of nanocapsules: Instability sources, formulation and process parameters, *Pharmaceutics*, 2021, **13**(8), 1112. Available from: <https://www.mdpi.com/1999-4923/13/8/1112>.
- 32 W. C. Luo, A. O. Beringhs, R. Kim, W. Zhang, S. M. Patel, R. H. Bogner, *et al.*, Impact of formulation on the quality and stability of freeze-dried nanoparticles, *Eur. J. Pharm. Biopharm.*, 2021, **169**, 256–267. Available from: <https://linkinghub.elsevier.com/retrieve/pii/S0939641121002691>.
- 33 M. S. Gatto and W. Najahi-Missaoui, Lyophilization of nanoparticles, does it really work? Overview of the current status and challenges, *Int. J. Mol. Sci.*, 2023, **24**(18), 14041. Available from: <https://www.mdpi.com/1422-0067/24/18/14041>.
- 34 A. Cherniienko, R. Lesyk, L. Zaprutko and A. Pawełczyk, IR-EcoSpectra: Exploring sustainable ex situ and in situ FTIR applications for green chemical and pharmaceutical analysis, *J. Pharm. Anal.*, 2024, **14**(9), 100951. Available from: <https://linkinghub.elsevier.com/retrieve/pii/S2095177924000480>.
- 35 Y. Gong, X. Chen and W. Wu, Application of fourier transform infrared (FTIR) spectroscopy in sample preparation: Material characterization and mechanism investigation, *Adv. Sample Prep.*, 2024, **11**, 100122. Available from: <https://linkinghub.elsevier.com/retrieve/pii/S2772582024000214>.
- 36 V. K. Chandur, T. Tk and A. R. Shabaraya, Comparative characterization of gel loaded ketoprofen nanosponges for topical delivery, *Int. J. Health Sci. Res.*, 2023, **13**(1), 44–58. Available from: https://www.ijhsr.org/IJHSR_Vol.13_Issue.1_Jan2023/IJHSR08.pdf.
- 37 S. A. Pullano, G. Marcianò, M. G. Bianco, G. Oliva, V. Rania, C. Vocca, *et al.*, FT-IR analysis of structural changes in ketoprofen lysine salt and KiOil caused by a pulsed magnetic field, *Bioengineering*, 2022, **9**(10), 503. Available from: <https://www.mdpi.com/2306-5354/9/10/503>.
- 38 F. Caputo, J. Clogston, L. Calzolari, M. Rösslein and A. Prina-Mello, Measuring particle size distribution of nanoparticle enabled medicinal products, the joint view of EUNCL and NCI-NCL. A step by step approach combining orthogonal measurements with increasing complexity, *J. Controlled Release*, 2019, **299**, 31–43. Available from: <https://linkinghub.elsevier.com/retrieve/pii/S0168365919301130>.
- 39 R. Muneer, M. R. Hashmet, P. Pourafshary and M. Shakeel, Unlocking the power of artificial intelligence: accurate zeta potential prediction using machine learning, *Nanomaterials*, 2023, **13**(7), 1209. Available from: <https://www.mdpi.com/2079-4991/13/7/1209>.
- 40 M. Sahimi, Characterization of Surface Morphology, in: *Heterogeneous Materials, Interdisciplinary Applied Mathematics*, Springer-Verlag, New York, 2003, vol. 23, pp. 5–22. Available from: https://link.springer.com/10.1007/0-387-21704-5_2.
- 41 L. García-Guzmán, G. Velazquez, I. Arzate-Vázquez, P. Castaño-Rivera, M. Guerra-Valle, J. Castaño, *et al.*, Preparation of nanocomposite biopolymer films from comelina coelestis willd starch and their nanostructures as a potential replacement for single-use polymers, *Foods*, 2024, **13**(24), 4129. Available from: <https://www.mdpi.com/2304-8158/13/24/4129>.
- 42 G. Maroli, V. Abarintos, A. Piper and A. Merkoçi, The clean-room-free, cheap, and rapid fabrication of nanoelectrodes with low zM limits of detection, *Small*, 2023, **19**(51), 2302136. Available from: <https://onlinelibrary.wiley.com/doi/10.1002/sml.202302136>.



- 43 P. Panwar, B. Pandey, P. C. Lakhera and K. P. Singh, Preparation, characterization, and in vitro release study of albendazole-encapsulated nanosize liposomes, *Int. J. Nanomed.*, 2010, **9**, 101–108.
- 44 A. Salt, A data set to verify volume and sample removal correction calculations for dissolution testing, *Dissolution Technol.*, 2021, **28**(2), 16–20. Available from: https://dissolutiontech.com/issues/202105/DT202105_A02.pdf.
- 45 K. A. Ali, R. Chakraborty, S. K. Roy and K. Ghosal, Design and development of ondansetron-loaded polysaccharide-based buoyant formulation for improved gastric retention and drug release, using both natural and semi-synthetic polymers, *Int. J. Biol. Macromol.*, 2025, 141105.
- 46 S. F. Diño, A. D. Edu, R. G. Francisco, E. Gutierrez, P. Crucis, A. M. Lapuz, *et al.*, Drug–excipient compatibility testing of cilostazol using FTIR and DSC analysis, *Philipp. J. Sci.*, 2023, **152**(6A), 2129–2137, Available from: <https://philjournalsci.dost.gov.ph/publication/regular-issues/past-issues/124-vol-152-no-6a-december-2023-part-a/1970-drug-excipient-compatibility-testing-of-cilostazol-using-ftir-and-dsc-analysis>.
- 47 S. A. Pullano, G. Marcianò, M. G. Bianco, G. Oliva, V. Rania, C. Vocca, *et al.*, FT-IR analysis of structural changes in ketoprofen lysine salt and KiOil caused by a pulsed magnetic field, *Bioengineering*, 2022, **9**(10), 503. Available from: <https://www.mdpi.com/2306-5354/9/10/503>.
- 48 K. A. Logacheva, A. V. Belushkin, P. A. Gergelezhiu, A. B. Eresko, S. N. Malakhov and E. V. Raksha, *et al.*, Molecular Mobility of Different Forms of Ketoprofen Based on DFT Calculation Data, in *ECSOC 2024*, MDPI, 2024, p. 60. Available from: <https://www.mdpi.com/2673-4583/16/1/60>.
- 49 P. Koczoń, J. T. Hołaj-Krzak, B. K. Palani, T. Bolewski, J. Dąbrowski, B. J. Bartyzel, *et al.*, The analytical possibilities of FT-IR spectroscopy powered by vibrating molecules, *Int. J. Mol. Sci.*, 2023, **24**(2), 1013. Available from: <https://www.mdpi.com/1422-0067/24/2/1013>.
- 50 S. Y. Lin, Current and potential applications of simultaneous DSC-FTIR microspectroscopy for pharmaceutical analysis, *J. Food Drug Anal.*, 2021, **29**(2), 182–202, Available from: <https://www.jfda-online.com/journal/vol29/iss2/1>.
- 51 S. Shen, Y. Wu, Y. Liu and D. Wu, High drug-loading nanomedicines: Progress, current status, and prospects, *Int. J. Nanomed.*, 2017, **12**, 4085–4109. Available from: <https://www.dovepress.com/high-drug-loading-nanomedicines-progress-current-status-and-prospects-peer-reviewed-article-IJN>.
- 52 Y. Liu, G. Yang, S. Jin, L. Xu and C. Zhao, Development of high-drug-loading nanoparticles, *ChemPlusChem*, 2020, **85**(9), 2143–2157. Available from: <https://chemistry-europe.onlinelibrary.wiley.com/doi/10.1002/cplu.202000496>.
- 53 J. P. Rao and K. E. Geckeler, Polymer nanoparticles: Preparation techniques and size-control parameters, *Prog. Polym. Sci.*, 2011, **36**(7), 887–913. Available from: <https://linkinghub.elsevier.com/retrieve/pii/S0079670011000232>.
- 54 F. Farjadian, A. Ghasemi, O. Gohari, A. Roointan, M. Karimi and M. R. Hamblin, Nanopharmaceuticals and nanomedicines currently on the market: Challenges and opportunities, *Nanomedicine*, 2019, **14**(1), 93–126. Available from: <https://www.tandfonline.com/doi/full/10.2217/nmm-2018-0120>.
- 55 L. Xu, X. Wang, Y. Liu, G. Yang, R. J. Falconer and C. X. Zhao, Lipid nanoparticles for drug delivery, *Adv. NanoBiomed Res.*, 2022, **2**(2), 2100109. Available from: <https://onlinelibrary.wiley.com/doi/10.1002/anbr.202100109>.
- 56 R. Vogel, A. K. Pal, S. Jambhrunkar, P. Patel, S. S. Thakur, E. Reátegui, *et al.*, High-resolution single particle zeta potential characterisation of biological nanoparticles using tunable resistive pulse sensing, *Sci. Rep.*, 2017, **7**(1), 17479.
- 57 E. Ponticorvo, M. Iuliano, C. Cirillo, A. Maiorino, C. Aprea and M. Sarno, Fouling behavior and dispersion stability of nanoparticle-based refrigeration fluid, *Energies*, 2022, **15**(9), 3059, Available from: <https://www.mdpi.com/1996-1073/15/9/3059>.
- 58 M. Laxmi, A. Bhardwaj, S. Mehta and A. Mehta, Development and characterization of nanoemulsion as carrier for the enhancement of bioavailability of artemether, *Artif. Cells, Nanomed., Biotechnol.*, 2015, **43**(5), 334–344. Available from: <https://www.tandfonline.com/doi/full/10.3109/21691401.2014.887018>.
- 59 M. HariPriyaa and K. Suthindhiran, Pharmacokinetics of nanoparticles: Current knowledge, future directions and its implications in drug delivery, *Future J. Pharm. Sci.*, 2023, **9**(1), 113, Available from: <https://fjps.springeropen.com/articles/10.1186/s43094-023-00569-y>.
- 60 Z. M. Mazayen, A. M. Ghoneim, R. S. Elbatanony, E. B. Basalious and E. R. Bendas, Pharmaceutical nanotechnology: From the bench to the market, *Future J. Pharm. Sci.*, 2022, **8**(1), 12, Available from: <https://fjps.springeropen.com/articles/10.1186/s43094-022-00400-0>.
- 61 J. Weng, H. H. Y. Tong and S. F. Chow, In vitro release study of the polymeric drug nanoparticles: Development and validation of a novel method, *Pharmaceutics*, 2020, **12**(8), 732, Available from: <https://www.mdpi.com/1999-4923/12/8/732>.
- 62 A. Elmaskaya, A. A. Ozturk, G. Buyukkoroglu and E. Yenilmez, Spray-dried ketoprofen lysine-incorporated PLGA nanoparticles; Formulation, characterization, evaluation and cytotoxic profile, *Pharm. Sci.*, 2019, **81**(4), 640–650, Available from: <https://www.ijpsonline.com/articles/spraydried-ketoprofen-lysineincorporated-plga-nanoparticles-formulation-characterization-evaluation-and-cytotoxic-profile-3665.html>.
- 63 J. Kluge, F. Fusaro, M. Mazzotti and G. Muhrer, Production of PLGA micro- and nanocomposites by supercritical fluid extraction of emulsions: II. Encapsulation of ketoprofen, *J. Supercrit. Fluids*, 2009, **50**(3), 336–343. Available from: <https://linkinghub.elsevier.com/retrieve/pii/S0896844609001697>.



- 64 P. P. Shah, P. R. Desai and M. Singh, Effect of oleic acid modified polymeric bilayered nanoparticles on percutaneous delivery of spantide II and ketoprofen, *J. Controlled Release*, 2012, **158**(2), 336–345. Available from: <https://linkinghub.elsevier.com/retrieve/pii/S0168365911010698>.
- 65 N. Varga, R. Béltéki, Á. Juhász and E. Csapó, Core-shell structured PLGA particles having highly controllable ketoprofen drug release, *Pharmaceutics*, 2023, **15**(5), 1355, Available from: <https://www.mdpi.com/1999-4923/15/5/1355>.
- 66 P. Kumar, A. L. Ganure, B. B. Subudhi and S. Shukla, Design and comparative evaluation of *in vitro* drug release, pharmacokinetics and gamma scintigraphic analysis of controlled release tablets using novel pH sensitive starch and modified starch-acrylate graft copolymer matrices, *Iran. J. Pharm. Res.*, 2015, **14**(3), 677–691.
- 67 Y. Fu and W. J. Kao, Drug release kinetics and transport mechanisms of non-degradable and degradable polymeric delivery systems, *Expert Opin. Drug Delivery*, 2010, **7**(4), 429–444. Available from: <https://www.tandfonline.com/doi/full/10.1517/17425241003602259>.
- 68 R. Batul, A. Khaliq, A. Alafnan, M. Bhave and A. Yu, Investigation of gentamicin release from polydopamine nanoparticles, *Appl. Sci.*, 2022, **12**(13), 6319. Available from: <https://www.mdpi.com/2076-3417/12/13/6319>.
- 69 P. Porbaha, R. Ansari, M. R. Kiafar, R. Bashiry, M. M. Khazaei, A. Dadbakhsh, *et al.*, A comparative mathematical analysis of drug release from lipid-based nanoparticles, *AAPS PharmSciTech*, 2024, **25**(7), 208. Available from: <https://link.springer.com/10.1208/s12249-024-02922-7>.
- 70 B. J. Lee, Y. Cheema, S. Bader and G. A. Duncan, Shaping nanoparticle diffusion through biological barriers to drug delivery, *JCIS Open*, 2021, **4**, 100025. Available from: <https://linkinghub.elsevier.com/retrieve/pii/S2666934X21000246>.
- 71 S. Borandeh, B. Van Bochove, A. Teotia and J. Seppälä, Polymeric drug delivery systems by additive manufacturing, *Adv. Drug Delivery Rev.*, 2021, **173**, 349–373. Available from: <https://linkinghub.elsevier.com/retrieve/pii/S0169409X21001010>.

